J. Earth Syst. Sci. (2023)132 67
https://doi.org/10.1007/s12040-023-02069-2

Opposite trends in heat waves and cold waves over India

Aninda Bhattacharya[1], Abin Thomas[1], Vijay K Soni[2], P S Roy[1], Chandan Sarangi[3,4] and Vijay P Kanawade[1,*]

[1]*Centre of Earth, Ocean and Atmospheric Sciences, University of Hyderabad, Hyderabad, India.*
[2]*India Meteorological Department, Ministry of Earth Sciences, New Delhi, India.*
[3]*Department of Civil Engineering, Indian Institute of Technology Madras, Chennai, India.*
[4]*Centre for Atmospheric and Climate Sciences, Indian Institute of Technology Madras, Chennai, India.*
**Corresponding author. e-mail: vijaykanawade03@yahoo.co.in*

MS received 15 August 2022; revised 15 November 2022; accepted 3 December 2022

Extreme weather events have become remarkably more evident in recent decades. Heat waves and cold waves are anomalous weather events resulting from excessive heat and cold conditions, respectively, in the near-surface atmosphere. They may last from a few days to a few weeks, depending on the geography and climatology of the region. In this study, we have used the India Meteorological Department (IMD) daily maximum and minimum temperature data over the period from 1970 to 2019 to investigate the decadal variability and trends in the frequency of heat waves and cold waves over the four broad climatic zones of India. We found opposite trends in the heat wave and cold wave events over India. The frequency of the occurrence of heat waves increased by about 0.6 events per decade, while cold waves decreased by about 0.4 events per decade. Although most of northwest India is highly vulnerable to heat wave conditions, central peninsular India is also experiencing frequent heat waves in the recent decade. Concurrently, the average duration of cold waves decreased over montane, arid and semi-arid, and tropical wet and dry climate zones. But, cold wave events frequency showed an increasing trend over the subtropical humid climatic zone of India. When compared to IMD observations, the CMIP6 models generally failed to capture the observed spatial features in the heat wave frequency trend and cold wave frequency trend. This suggests that CMIP6 model output data should be used cautiously to predict future changes in the heat wave and cold wave events frequency. This emphasizes the need for an improved process-level understanding of these extreme events.

Keywords. Extreme weather events; heat waves; cold waves; climate data.

1. Introduction

Heat waves and cold waves are anomalous extreme weather phenomena that have been widely studied in recent decades due to their severe adverse impacts on agriculture, human health, and industrial production (Fu *et al.* 2018; Piticar *et al.* 2018; Cheng *et al.* 2019; Ray *et al.* 2021). The latest sixth assessment report of the IPCC suggests that the frequency and intensity of extreme weather events, such as heat waves, have increased over Southeast Asia, while the frequency and intensity of cold waves have decreased at a high confidence level (IPCC 2021).

Numerous studies have reported the increasing trend in heat waves and their associated impacts

Supplementary materials pertaining to this article are available on the *Journal of Earth System Science* website (http://www.ias.ac.in/Journals/Journal_of_Earth_System_Science).

Published online: 10 April 2023

on India (Ratnam *et al.* 2016; Rohini *et al.* 2016; Mazdiyasni *et al.* 2017; Dave *et al.* 2020; Mondal *et al.* 2021; Ray *et al.* 2021). Ratnam *et al.* (2016) suggested that there are two types of heat waves based on the maximum temperature variability; the first type of heat waves over north-central India is associated with the modification of the zonal atmospheric circulation, which causes subsidence over the Indian region referred to as blocking events over the north Atlantic. The second type of heat wave observed over coastal eastern India was due to the anomalous Matsuno-Gill response to the cooling in the Pacific Ocean. Severe heat waves are projected to rise 30 times by the end of the 21st century for a world with a global mean temperature of 2°C above pre-industrial times (Mishra *et al.* 2017). De *et al.* (1998) linked severe heat waves to one of the strongest 1998 El Niño of the twentieth century. Jenamani (2012) suggested that the variation in the sea surface temperature in the Bay of Bengal can hinder the onset of sea breeze and may cause heat waves in coastal regions. A recent study also showed that the western Indian Ocean (1.2–1.5 events per decade) and the Bay of Bengal (0.4–0.5 events per decade) observed an increasing trend in marine heat waves (Saranya *et al.* 2022).

When it comes to cold waves, it has been well established that the trend in the spatial and temporal distribution of cold waves is decreasing over major parts of the continents across the globe due to anthropogenic warming. Most studies have confirmed that the occurrence of cold days and nights is decreasing (Lu *et al.* 2015; Spinoni *et al.* 2015; Unkašević and Tošić 2015; Piticar *et al.* 2018; Bitencourt *et al.* 2020; Namroodi *et al.* 2021). Van Oldenborgh *et al.* (2019) revealed that cold waves are getting milder, especially over northern mid-latitudes, due to warming associated with increasing greenhouse gas emissions. In contrast, Ma *et al.* (2019) suggest that Arctic warming increases the occurrence of East Asian severe cold waves by inducing larger internal atmospheric variability. Lu *et al.* (2015) also showed the highest temperature drops (>9°C) over Western Siberia and Central Siberia and the other near Alaska region encompassing some parts of the United States.

In the Indian context, there are a scanty number of studies investigating cold waves compared to heat waves. Cold and dry air from the northern latitudes, particularly during the passage of transient systems, can cause a change in the observed wind and precipitation patterns in the north, north-western and central parts of India, resulting in cold wave (CW) events during the winter season (Pai *et al.* 2022). Further, the phases of El Niño Southern Oscillation (ENSO) can create a favourable environment for cold waves during boreal winters. Ratnam *et al.* (2016) showed that the CW events with relatively colder temperatures covering most parts of India are associated with the cooling phase of the ENSO (La Niña) whereas the CW events over north-western India with anomalously cold temperatures can be associated with the warming phase of the ENSO (El Niño). Few studies, such as Pai *et al.* (2017) and Dash *et al.* (2011), have reported the decreasing trend in cold waves over India. While Bhatla *et al.* (2020) reported a high frequency of the cold wave and severe cold wave events over the Indo-Gangetic Plain (IGP) during December and January. Mahdi *et al.* (2016) have reported a decreasing trend in cold waves over the eastern IGP (Bihar). Thus, even though the frequency and intensity of cold waves are decreasing in most countries, it warrants more observational studies for better quantification. Therefore, our understanding of the temporal and spatial scale of cold waves over India and heat waves to a certain extent has not yet been fully explored. Such extreme events may last from a few days to a few weeks, depending on the region's geographic setting and climate type. On average, heat wave events last for about 5–6 days (Rohini *et al.* 2016), whereas the duration of a cold wave event is about 9–10 days in north-western India (Sandeep *et al.* 2020).

Most of the recent studies using CMIP5 and CMIP6 model data have tried to capture the future projections of heat wave conditions over India. Das *et al.* (2022) have used 26 GCM model data to identify the future implications of heat wave conditions over India. Under the RCP8.5 scenario, more intense heat wave episodes are expected to rise. Chowdhury (2022) suggests the high amplification of heat wave density as compared to heat wave frequency by the latter half of the century over India. Mishra *et al.* (2017) showed that by the end of the twenty-first century, the frequency of severe heat waves would likely increase by 30 times for 2°C warming if there were no reduction measures. Kumar *et al.* (2019) evaluated the CMIP5 model's performance to examine the historical surface temperature scenario over India during 1971–2005. In contrast, there is a lack of studies using GCM model data that analyze the future cold wave projections over India.

In this study, we have used the India Meteorological Department (IMD) gridded daily maximum and minimum temperature data from 1970 to 2019 to determine the temperature anomalies and decadal trend in frequency, intensity, and duration of occurrence of heat waves and cold waves in various climatic zones of India. There is no universal criterion for determining heat waves or cold waves. We have used the widely accepted metric of excess heat factor (EHF) and excess cold factor (ECF) based on Nairn *et al.* (2015), which provides a spatially and temporally comparable metric, considering both magnitude and duration of anomalously high and low-temperature days for the heat wave and cold wave events, respectively. Then we compared the spatial trend in the heat wave (HW) and cold wave (CW) intensity and frequency with thirteen GCM members of CMIP6 model data to check whether the models captures the observed trend.

2. Materials and methods

2.1 *Study region*

India experiences a tropical monsoon climate with a wide range of regional variations throughout the year. Köppen-Geiger's classification roughly divides India into six climatic zones with minor divisions, especially over North India. Here, we have used a modified version of this classification to divide India approximately into four broad climatic zones (figure 1) namely, (i) montane – encompassing the alpine climate in the northern states such as Ladakh, Jammu and Kashmir, Himachal Pradesh and some parts of Uttarakhand, Sikkim and Arunachal Pradesh; (ii) arid and semi-arid – comprising the dry climate of Rajasthan and semi-arid climate of Gujarat; (iii) humid subtropical – most of the Indo-Gangetic basin such as Bihar, Jharkhand and Chhattisgarh, Uttar Pradesh and West Bengal and some parts of Madhya Pradesh and north-eastern subtropical highlands of Assam, Nagaland, and a majority of other north-eastern states which subjected to warm and hot summers with high humidity and with ample rainfall during monsoon season; and (iv) tropical wet and dry – encompassing the southern peninsular India where the majority of regions have a tropical dry and wet climate. According to Köppen-Geiger's classification, a small portion of the southern peninsula is semi-arid, and some of the eastern hilly regions are alpine in nature.

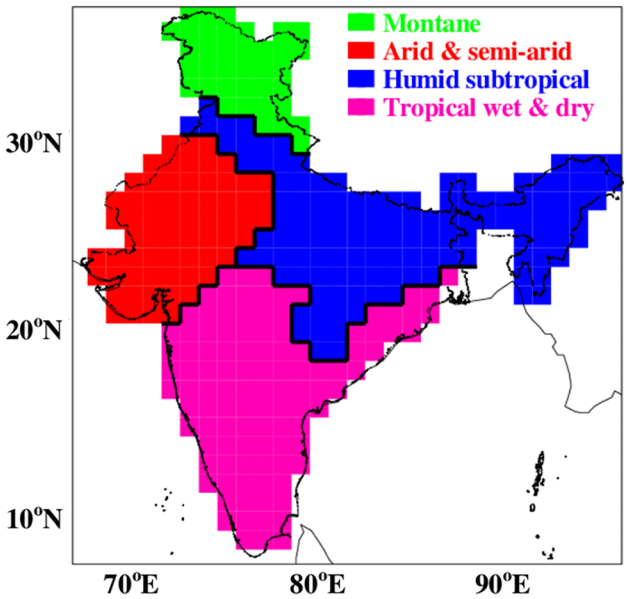

Figure 1. The climatic zones of India that are considered in this study based on a modified version of Koeppen's climate classification.

However, to reduce uncertainty in our analysis, these minor divisions have been neglected in the analysis.

2.2 *IMD gridded temperature data*

The 1° × 1° gridded daily maximum (T_{MAX}), mean (T_{MEAN}), and minimum (T_{MIN}) temperature data for the period of 1970–2019 from the India Meteorological Department was used in this study (Srivastava *et al.* 2009). Before gridding, the station data was subjected to numerous quality checks, including homogeneity checks. Furthermore, only stations with more than ten years of data and a minimum of 300 days per year were included in this study in the creation of this product. Using temperature data from 395 quality-controlled stations, a high-resolution daily gridded temperature data set for the Indian region was created. For interpolating the station temperature data into 1° latitude and 1° longitude grids, a modified version of Shepard's angular distance weighting algorithm was used. A cross-validation error estimation technique was used to estimate errors, which were found to be less than 0.5°C. The data set was also compared to other high-resolution data sets, which were also found to be comparable. Daily temperature anomalies were used instead of absolute values to avoid biases during gridding. The above data set was obtained from the Climate Services Division archive at IMD, Pune.

2.3 *CMIP6 temperature data*

The latest version of coupled model intercomparison project (CMIP6) has 51 global coupled ocean-atmospheric models in its historical run (1850–2014) of daily temperature data. The historical run is based on historical greenhouse gas concentrations, aerosols, radiative effects, and solar irradiance data. In this study, we have used 13 models (table 1). The bias-corrected datasets were developed by Mishra *et al.* (2020) at 0.25° resolution. Bias-corrected maximum and minimum temperature data for India was downloaded and re-gridded in a 1° × 1° grid to match IMD observations. The data from 1970–2014 in the historical simulation is used in this analysis to compare with IMD observational data.

2.4 *Heat wave and cold wave index calculations*

We have used EHF for heat waves and ECF for cold waves, originally developed by Nairn *et al.* (2015). EHF and ECF use daily maximum temperature (T_{MAX}) and minimum temperature (T_{MIN}) values. The daily mean temperature (DMT, T_i) is calculated as the average of T_{MAX} and T_{MIN}, i.e., $(T_{\mathrm{MAX}} + T_{\mathrm{MIN}})/2$. It should be noted that EHF-based indices were analyzed for the summer months of April through June, whereas ECF-based indices were analyzed for the winter months of December through February during the period 1970–2019.

EHF is based on two excess heat indices, namely heat stress and excess heat ($\mathrm{EHI}_{(accl)}$). The excess heat index ($\mathrm{EHI}_{(sig)}$) measures the abnormally high heat that arises from a high daytime temperature that is not adequately discharged during the night due to unusually higher night-time minimum temperatures. The daily mean temperature (DMT) is calculated for a three-day time window and compared against a climate reference value (T_{95}, climatological mean of 95th percentile values of DMT for the climate reference period of 1970–1999) to acquire the value of $\mathrm{EHI}_{(sig)}$ and mathematically expressed as:

$$\mathrm{EHI}_{(sig)} = \frac{(T_i + T_{i-1} + T_{i-2})}{3} - T_{95}, \qquad (1)$$

$\mathrm{EHI}_{(sig)}$ is calculated in °C.

The component of heat stress (Rohini *et al.* 2016) arises from the difference in temperature of the warm day compared to the recorded average temperature of the recent past. Subsequent maximum and minimum temperatures averaged over a three-day period and the previous 30 days are compared to determine heat stress. It is mathematically expressed as:

$$\mathrm{EHI}_{(accl)} = \frac{(T_i + T_{i-1} + T_{i-2})}{3} - \frac{(T_{i-3} + \cdots + T_{i-32})}{30}. \qquad (2)$$

$\mathrm{EHI}_{(accl)}$ is essentially the difference of three-day DMT compared to the previous 30 days. The unit of $\mathrm{EHI}_{(accl)}$ is calculated in °C.

Equations (1) and (2) are then combined to determine EHF given as,

Table 1. *List of CMIP6 models considered in this study.*

Sl. no.	Model name	Institution
1	ACCESS-CM2	CSIRO, Australian Research Council Centre of Excellence for Climate System Science (ACCESS)
2	ACCESS-ESM 1-5	Commonwealth Scientific and Industrial Research Organization, Australia
3	BCC-CSM2-MR	Beijing Climate Center, China Meteorological Administration, China
4	CanESM5	Canadian Centre for Climate Modelling and Analysis, Canada
5	EC-Earth3	EC-EARTH consortium
6	EC-Earth3-Veg	EC-EARTH consortium
7	INM-CM4-8	Institute for Numerical Mathematics (INM), Russia
8	INM-CM5-0	Institute for Numerical Mathematics (INM), Russia
9	MPI-ESM 1-2-HR	Max Planck Institute for Meteorology, Deutscher Wetterdienst, Deutsches Klimarechenzentrum, Germany
10	MPI-ESM 1-2-LR	Max Planck Institute for Meteorology, Alfred Wegener Institute, Germany
11	MRI-ESM 2-0	Max Planck Institute for Meteorology, Alfred Wegener Institute, Germany
12	NorESM2-LM	Norwegian Climate Centre, Norway
13	NorESM2-MM	Norwegian Climate Centre, Norway

$$\mathrm{EHF} = \mathrm{EHI}_{(sig)} \times \max\left(1, \mathrm{EHI}_{(accl)}\right). \quad (3)$$

The unit of EHF is $(°C)^2$.

Similarly, the ECF can be calculated as,

$$\mathrm{ECF} = -\mathrm{ECI}_{(sig)} \times \min\left(-1, \mathrm{ECI}_{(accl)}\right), \quad (4)$$

where $\mathrm{ECI}_{(sig)}$ is the excess cold index, and $\mathrm{ECI}_{(accl)}$ is excess cold acclimatization. The positive value of EHF is indicative of the heat wave condition while the negative value of ECF is indicative of the cold wave condition. The more the positive value of EHF, the more severe the heat wave, and the lesser the negative value of ECF, the more severe the cold wave. Here, we considered EHF values greater than the 75th percentile value of EHF ($\mathrm{EHF}_{75\mathrm{p}} = 2.61°C^2$) to identify moderate to severe heat wave events while ECF values less than the 25th percentile value of ECF ($\mathrm{ECF}_{25\mathrm{p}} = -3.50°C^2$) to identify moderate to severe cold wave events. Supplementary table S1 summarises EHF and ECF calculated threshold values for identifying heat waves and cold waves for IMD observational data and CMIP6 models.

3. Results and discussion

3.1 *Trends in the anomaly of maximum and minimum temperature*

Figure 2 shows the yearly trend in the anomaly of daily maximum temperature over the four climatic zones from 1970 to 2019 in India. The anomaly in daily maximum temperature shows large inter-annual variability (standard deviation = 0.35°C), with an increasing trend in all four climatic zones. Overall, the mean increase in the daily maximum temperature anomaly over India was ∼0.72 to 0.77°C in the last 50 years, with peak enhancement over the tropical wet and dry zone, where T_{MAX} increased by about 0.77 ± 0.03°C. The montane, humid subtropical, and arid and semi-arid zones showed an anomalous increase in the daily maximum temperature by about 0.68 ± 0.03°C, 0.61 ± 0.03°C, and 0.71 ± 0.03°C, respectively, over the same time period.

Figure 3 shows the yearly trend in the mean anomaly of the daily minimum temperature over each climatic zone during the study period from 1970 to 2019. The anomalous increase in T_{MIN} is consistent with the anomalous increase in T_{MAX}, but the largest increase in the anomaly of T_{MIN} was observed for the arid and semi-arid zone, with T_{MIN} increasing by about 1.33 ± 0.04°C in the last 50 years (1970–2019). The montane, humid subtropical, and tropical wet and dry zones showed an anomalous increase in the daily minimum temperature by about 0.73 ± 0.03°C, 0.67 ± 0.02°C, and 0.37 ± 0.02°C, respectively, over the same time period.

The yearly anomaly of the daily mean temperature is also shown in Supplementary figure S1. The arid and semi-arid zone shows the highest T_{MEAN} anomaly for the same study period whereas, the tropical wet and dry zone shows the least increase in T_{MEAN}.

3.2 *Trends in heat waves and cold waves*

Such anomalous increases in T_{MAX} and T_{MIN} could lead to extreme heat stress. We quantified the intensity of the heat wave and cold wave by calculating the heat (or chill) coefficients, i.e., EHF and ECF, respectively. The higher positive (negative) values of EHF (ECF) indicate the more severe heat wave (cold wave) events. In this study, days with the absolute intensity of the EHF and ECF values >2 and the overall duration of this intensity persisted for at least three consecutive days were identified as heat wave and cold wave events, respectively.

Figure 4 shows the spatial distribution of climatological trend EHF over India averaged over the time period from 1970 to 2019 and the bar plot of the decadal mean EHF for each climatic zone. The spatial trend in EHF shows an increase over relatively arid regions of Rajasthan state and other north-western states of India, extending a tone of higher values to central-eastern-peninsular India. This clearly resembles its obvious dependence on daily temperature variability. The extreme north and north-western parts experience high daily temperature variability mainly due to their higher latitude, altitude, and distance from the sea. The decadal mean EHF for arid and montane regions is the highest in recent years, while tropical wet and dry, and subtropical humid show a decreasing trend in EHF values.

Figure 5 shows the spatial trend in ECF over India averaged over the time period from 1970 to 2019 and the bar plot of the decadal mean ECF for each climatic zone. The spatial trend shows the highest decrease in ECF over relatively humid subtropical regions of Uttar Pradesh state and an increase in ECF over arid and semi-arid regions of north-western states such as Rajasthan extending to the northern montane states of Jammu and

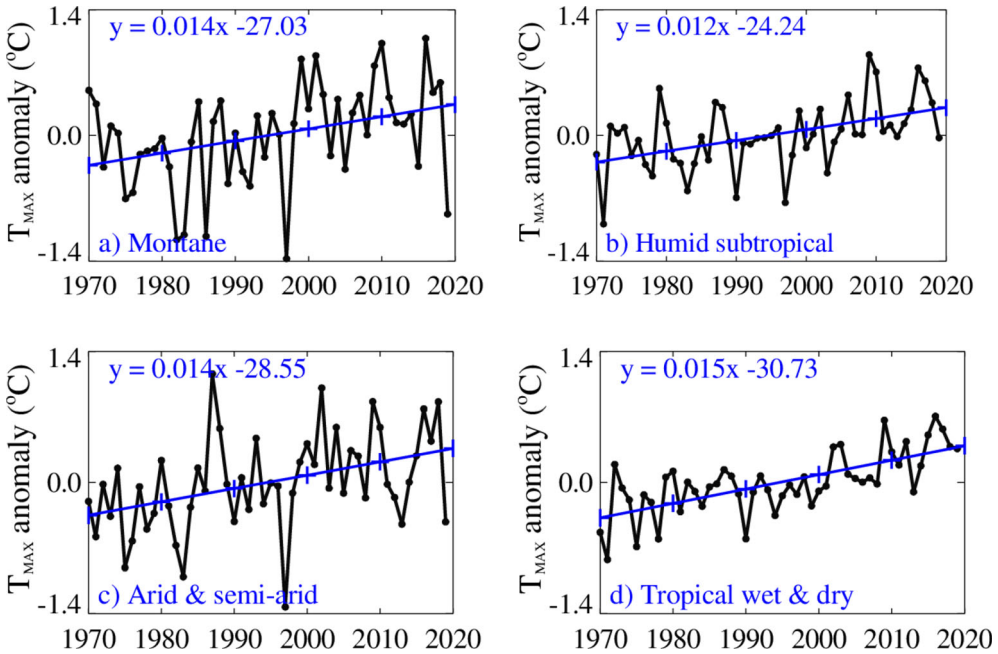

Figure 2. The yearly anomaly of daily maximum temperature over different climatic zones during the study period 1970–2019. The trend (°C/year) is significant at a 95% confidence interval.

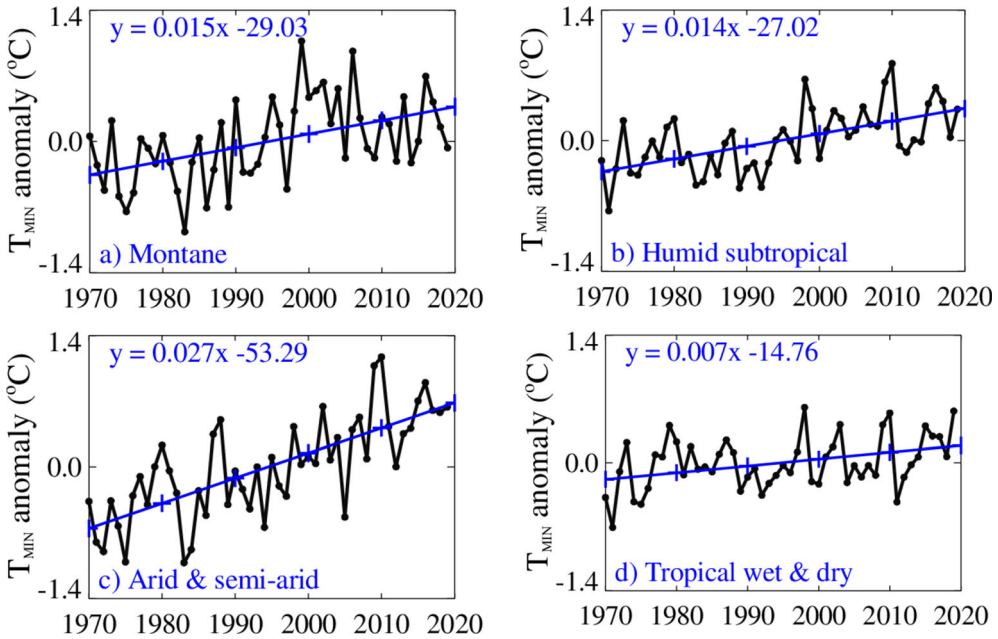

Figure 3. The yearly anomaly of daily minimum temperature over each climatic zone during the study period 1970–2019. The trend (°C/year) is significant at a 95% confidence interval.

Kashmir. The increasing trend in ECF can be correlated with the decrease in the severity of cold wave events and vice versa as ECF values lie between $(-2, -\infty)$. There is an overall increase in ECF values over the years observed for arid and montane regions indicating the possible decrease in the severity of severe cold wave events in the region. However, for the tropical wet and dry zone, the ECF values are significantly lower indicating increased severity of cold waves. ECF values decreased almost two-fold over the humid subtropical zone from 1970–2019 indicating the high increase in the severity of cold wave events over the region. For tropical wet and dry zone, there is no significant change in spatio-temporal variability in the severity of cold wave events.

Figure 6 shows the spatial trend in HW frequency obtained over the time period from 1970 to

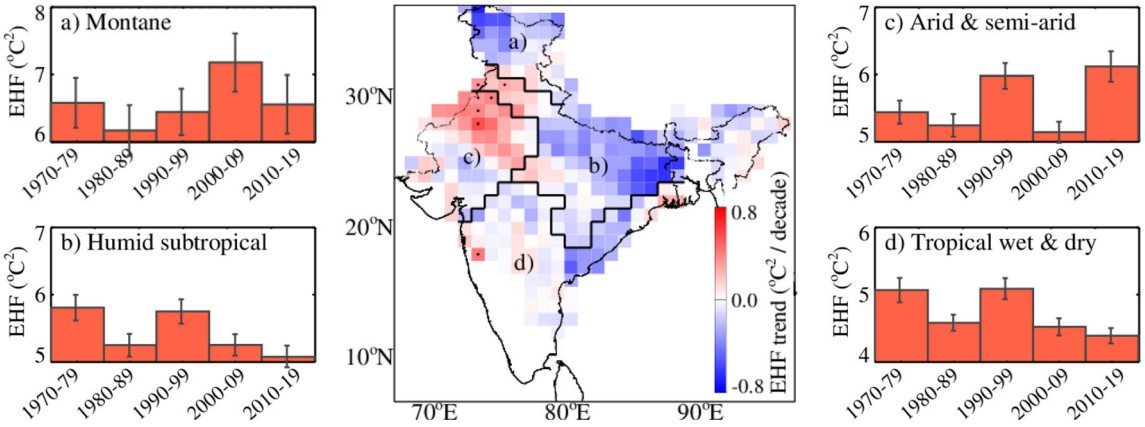

Figure 4. Spatial distribution of trend in EHF over India based on 1970–2019 time period and bar plots showing decadal mean EHF for four climatic zones, i.e., (**a**) montane; (**b**) humid subtropical; (**c**) arid and semi-arid and (**d**) tropical wet and dry zones.

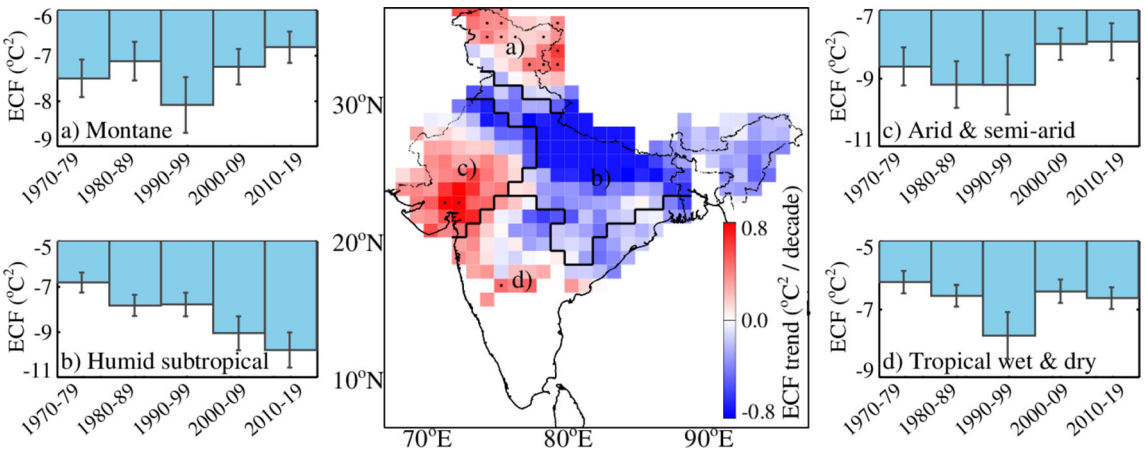

Figure 5. Spatial distribution of trend in ECF over India based on 1970–2019 time period and bar plots showing decadal mean ECF for four climatic zones, i.e., (**a**) montane; (**b**) humid subtropical; (**c**) arid and semi-arid and (**d**) tropical wet and dry zones.

2019 over India and the mean decadal HW frequency for each climatic zone. The HW event frequency over arid and semi-arid and tropical wet and dry zones shows an increasing trend. The arid zone experienced about 0.92 heat waves per decade during 1970–1979, which has increased to about 1.70 events/decade during 2010–2019. Compared to this, tropical wet and dry zone experienced about 0.82 HW events/decade during 1970–1979, which has increased to 1.07 events/decade during 2010–2019. In contrast, HW frequency over the subtropical humid region showed a decreasing trend during 1970–2009 from 1.73 events/decade to 1.27 events/decade. However, the same increased during 2010–2019 to about 1.69 events/decade. Montane zone showed a consistently decreasing trend in the frequency of heat waves from 2.05 events/decade from 1970 to 1979 to 0.84 events/decade from 2010 to 2019.

Figure 7 shows the spatial trend in cold wave event frequency over India during 1970–2019 and the decadal mean CW frequency for each climatic zone. The CW frequency clearly shows a decreasing trend over arid and semi-arid zone from 3.8 events/decade from 1970 to 1979 to about 2.85 events/decade from 2010 to 2019. Montane zone also showed decreasing trend from about 3.05 CW events/decade during 1970–1979 to about 2.16 events/decade during 2010–2019. Tropical wet and dry zone also showed a decreasing trend in CW frequency from 2.05 events/decade from 1970 to 1979 to 1.42 events/decade from 2010 to 2019. However, the subtropical humid zone showed a slight increase in CW event frequency from about 2.42 events/decade during 1970–1979 to 2.64 events/decade during 2010–2019.

3.3 *Trends in heat and cold waves as observed from CMIP6 historical data*

The spatial correlation between IMD data and CMIP6 historical data was performed. Overall,

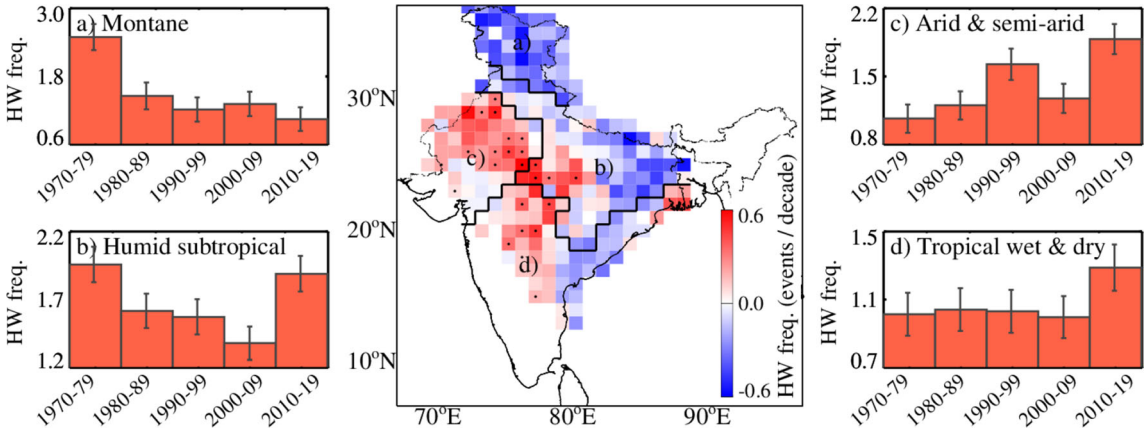

Figure 6. Spatial distribution of trend in HW frequency over India based on 1970–2019 time period and bar plot showing decadal mean HW frequency over each of the four climatic zones, i.e., (**a**) montane; (**b**) humid subtropical; (**c**) arid and semi-arid and (**d**) tropical wet and dry zones. The black dots represent statistical significance obtained using Student's *t*-test at a confidence interval of 90%.

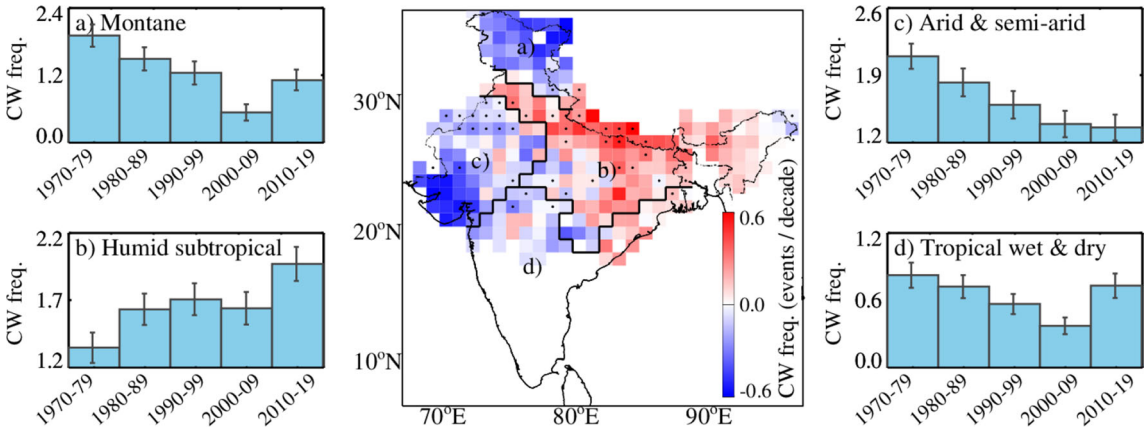

Figure 7. Spatial distribution of trend in CW frequency over India based on 1970–2019 time periods and bar plot showing the mean decadal average of CW event frequency over each of the four climatic zones, i.e., (**a**) montane; (**b**) humid subtropical; (**c**) arid and semi-arid and (**d**) tropical wet and dry zones. The black dots indicate the statistical significance obtained using Student's *t*-test at a confidence interval of 90%. The error bars indicate the 90% confidence interval of the mean CW event frequency standard deviation.

there is a strong correlation between CMIP6 temperature and IMD temperature data (figures S1–S4). Figure 8 shows the spatial distribution of trends in EHF over India. Most CMIP6 models captured the increasing trend in EHF over the arid and semi-arid zone. ACCESS-CM2 (figure 8a) is showing an increasing trend in EHF throughout all four zones with the highest significance while MPI-ESM 1-2 HR (figure 8i) showed a decreasing trend in EHF over most parts of India. Only EC-Earth3 (figure 8e) compares reasonably well with IMD observation (figure 8o). Nor-ESM2 MM (figure 8m) can capture positive and negative trends over arid and semi-arid climatic zone but failed to capture decreasing trends in EHF over humid subtropical climate zone. The ensemble of 13 CMIP6 models (figure 8n) shows an increasing trend throughout all four zones and the increasing trend in EHF over the arid and semi-arid zone is underestimated. When it comes to ECF, none of the CMIP6 models capture the spatial distribution of trends (figure 9). While CanESM5 (figure 9d), EC-Earth3-Veg (figure 9f), INM-CM5-0 (figure 9h), MRI-ESM 2-0 (figure 9k), NorESM2-MM (figure 9m) displayed increasing trends in ECF over the arid and semi-arid zone, similar to IMD observation (figure 9o), but these models failed to capture decreasing trend in ECF over the humid subtropical zone. The trend in the ensemble of 13 CMIP6 models (figure 9n) was significantly underestimated over the arid and semi-arid zone and failed to capture the decreasing trend over the humid subtropical zone when compared with IMD observations.

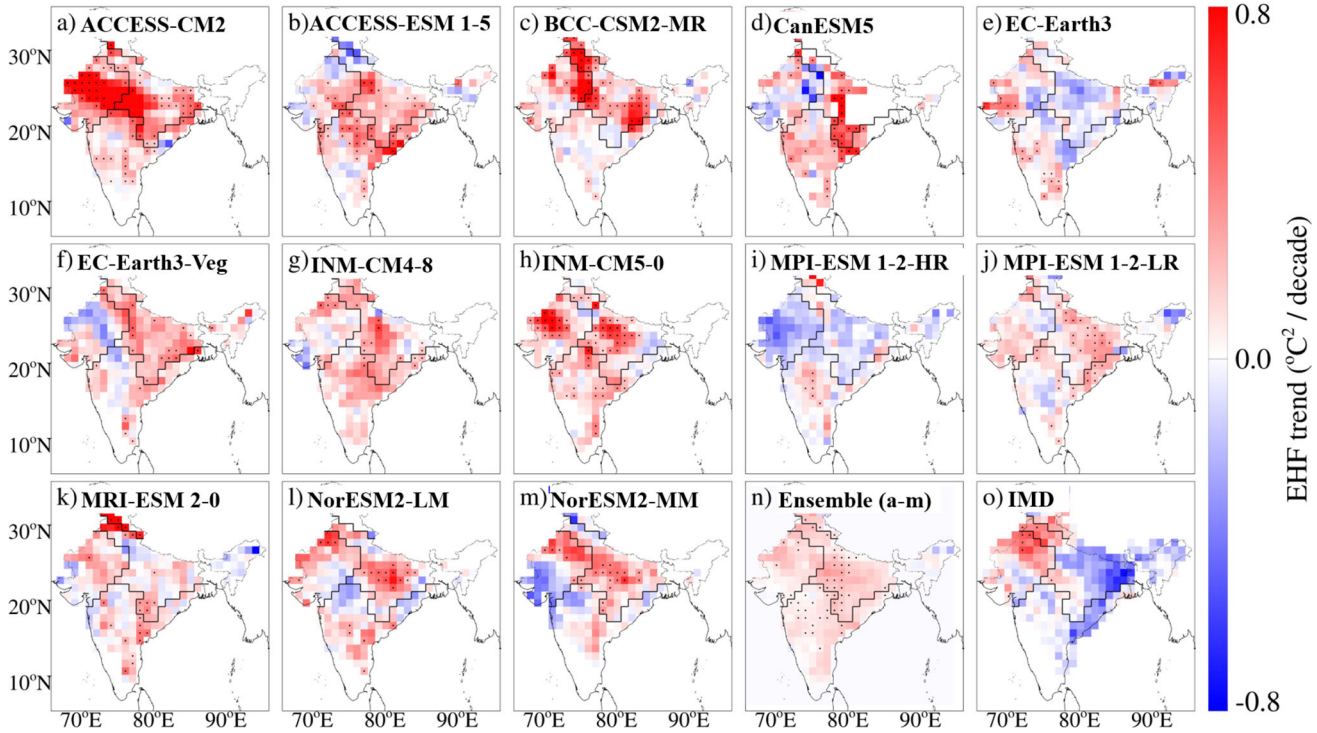

Figure 8. Spatial distribution of trend in EHF intensity over India based on 1970–2014 time period for (**a–m**) 13 CMIP6 historical simulations, (**n**) ensemble of 13 historical simulations, and (**o**) IMD observational data. The black dots indicate the statistical significance obtained using Student's *t*-test at a confidence interval of 95%.

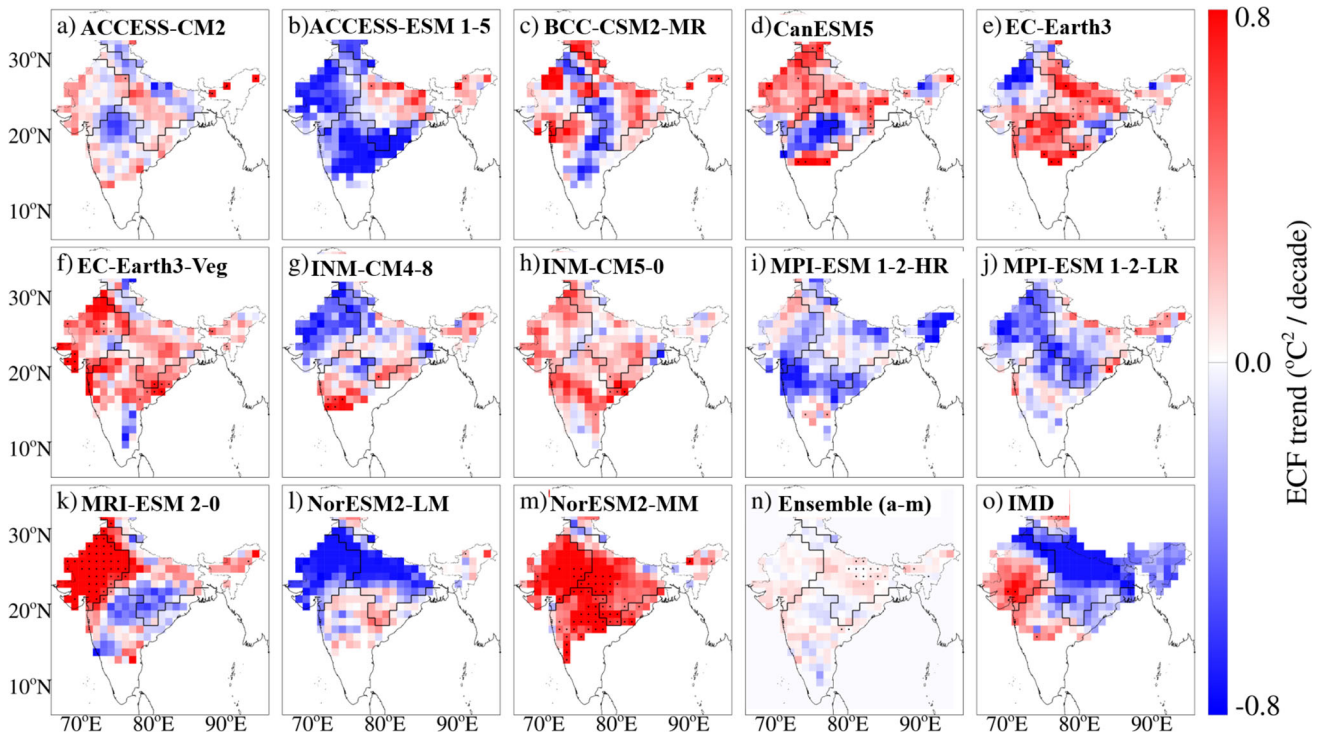

Figure 9. Spatial distribution of trend in ECF intensity over India based on 1970–2014 time period for (**a–m**) 13 CMIP6 historical simulations, (**n**) ensemble of 13 historical simulations, and (**o**) IMD observational data. The black dots indicate the statistical significance obtained using Student's *t*-test at a confidence interval of 95%.

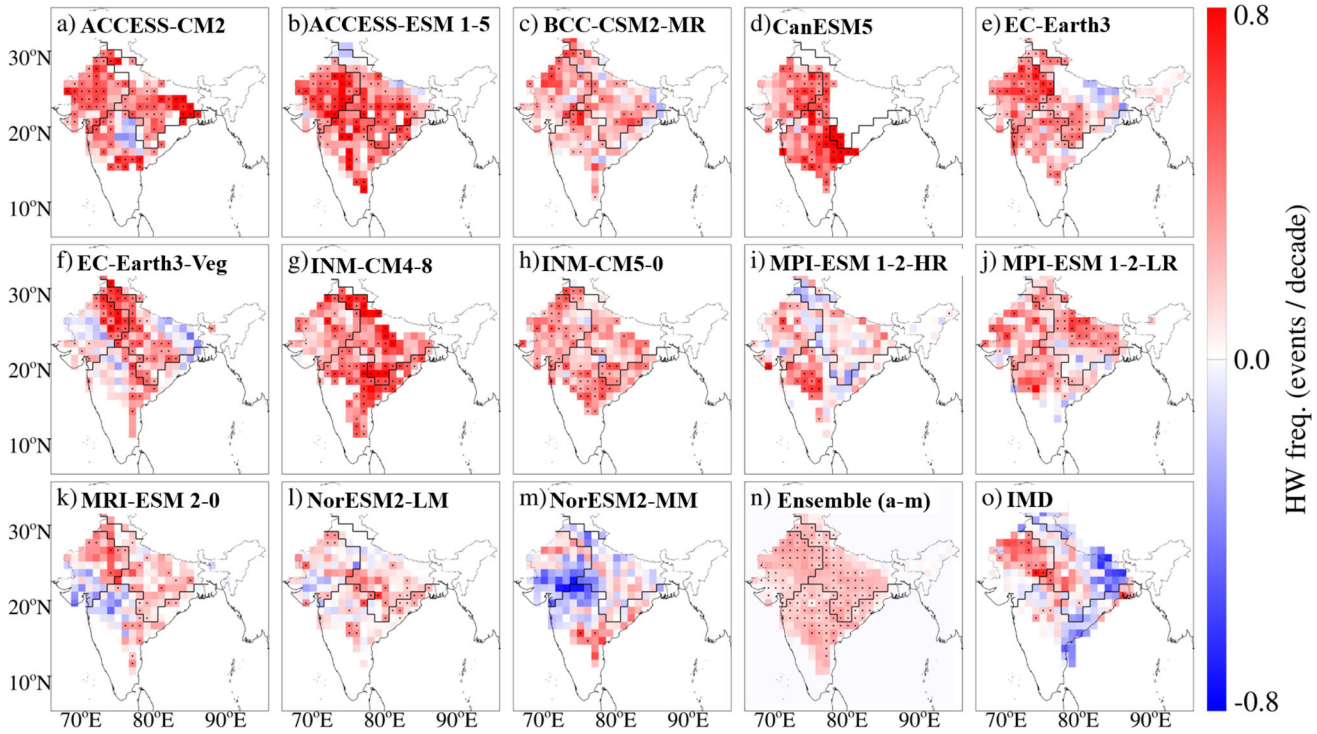

Figure 10. Spatial distribution of trend in HW frequency over India based on 1970–2014 time period for (**a–m**) 13 CMIP6 historical simulations, (**n**) ensemble of 13 historical simulations, and (**o**) IMD observational data. The black dots indicate the statistical significance obtained using Student's *t*-test at a confidence interval of 95%.

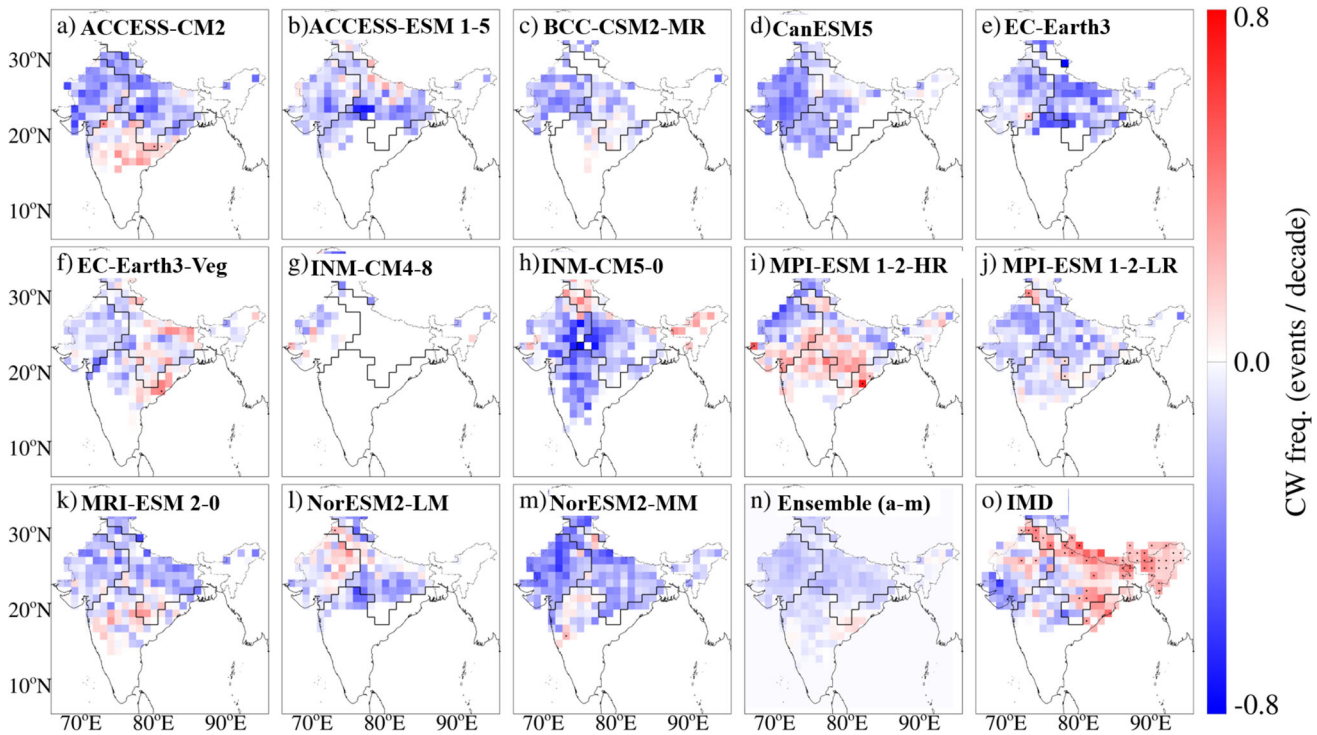

Figure 11. Spatial distribution of trend in CW frequency over India based on 1970–2014 time period for (**a–m**) 13 CMIP6 historical simulations, (**n**) ensemble of 13 historical simulations, and (**o**) IMD observational data. The black dots indicate the statistical significance obtained using Student's *t*-test at a confidence interval of 95%.

The increase in the decadal HW frequency over northwest and central India was observed in IMD data (figure 6). Here we look at how it has been reflected by the global circulation models from the CMIP6 (figure 10). When compared to IMD observations, almost all models failed to capture

the observed decreasing trend in HW frequency over the humid subtropical zone and some parts of the montane zone, except EC-Earth3 (figure 10e) scarcely showing a decreasing trend in HW frequency over the eastern humid subtropical zone. However, all models capture the observed increasing trend in HW frequency over the arid and semi-arid zone, except NorESM2-MM (figure 10m). Our findings are also consistent with earlier research, including that by Hirsch *et al.* (2021), which found that historical runs of the CMIP6 models for the years 1950–2014 underestimated heat wave frequency globally (figure 10n), while the ensemble of 13 historical simulations failed to capture the decreasing trend over the eastern humid subtropical zone. Similarly, almost all models failed to capture the observed increasing trend in cold wave frequency over the humid subtropical zone (figure 11o), except MPI-ESM 1-2 HR (figure 11i) barely captures an increasing trend over the humid subtropical zone. Further, the ensemble of 13 historical simulations also showed a decreasing trend in cold wave frequency over the arid and semi-arid zone, but it is generally underestimated when compared with IMD observations.

4. Summary

The daily maximum and minimum temperature anomalies show a consistent increase over the years in each and every climatic zone during 1970–2019, clearly indicating warming over the years. The T_{MAX} anomalies show a consistent increase overall in each of the four climatic zones of about 0.012–0.015°C per year. However, there is a significantly higher T_{MIN} anomaly observed for the arid and semi-arid zone of about 0.027°C per year, whereas the observed anomalies over the tropical wet and dry regions are significantly lower, about 0.007°C per year.

There has been a gradual increase (decrease) in the severe heat wave (cold wave) events over most of India during the recent decades due to anthropogenic warming. Our results are quite similar to the ones previously obtained by Pai *et al.* (2017) and Rohini *et al.* (2016). However, an overall increase or decrease in such events does not give away the exact picture. The montane zone showed a decrease in the number of severe heat wave events, whereas the humid subtropical zone showed a gradual increase in extreme cold wave events. The decreasing trend in heat wave events over the montane zone is insignificant, which can be attributed to the lack of observation data points over the region. However, there is a decrease in the frequency of HW events over the humid subtropical region at a 90% confidence level from 1.73 events/decade to 1.27 events/decade during 1970–2009.

The increase in severity and the number of cold wave events over the humid subtropical zone can be attributed to the high number of cold wave events during December and January over the IGP region (Bhatla *et al.* 2020). There can be a possible influence on the cold wave pattern due to the significant accumulation of aerosols over the region during dry months (Babu *et al.* 2013). Thomas *et al.* (2019) also reported that there had been a rise in winter hazy days over Central India at a rate of 2.6 days/year approximately compared to 1.7 days/year observed for IGP overall due to the consistent increase in accumulation of absorbing aerosols over the region. Also, the changing trend of western disturbances might affect the cold wave patterns (Hunt *et al.* 2019). The western disturbance systems bring rain to these regions during the winter months to IGP (Dimri *et al.* 2014). There is a significant temperature drop observed after the precipitation events over these regions.

Furthermore, our results suggest that the CMIP6 models do not adequately capture the spatial variability of heat waves and cold waves intensity and frequency over India. When compared to IMD observations in all four climatic zones, the CMIP6 models generally failed to capture the observed spatial features in the heat wave frequency trend and cold wave frequency trend. While the trends in heat wave frequency and cold wave frequency based on multi-model mean of the thirteen models matches with IMD observations over the arid and semi-arid zone, they are underestimated significantly.

Acknowledgements

The authors are thankful to the India Meteorological Department, Ministry of Earth Sciences, for providing daily gridded temperature data. VPK would like to thank the University Grants Commission, Government of India for the UGC-Faculty Recharge Programme Fellowship [Ref. No. F.4-5(230-FRP/2015/BSR)]. AT was supported by University Grants Commission Junior Research Fellowship. The authors are thankful to

anonymous reviewers for constructive comments and suggestions.

Author statement

VPK and CS conceptualized and designed the study, AB and AT performed data analysis and interpretation with critical inputs from VPK and CS. VKS and PSR provided the required resources. AB wrote the first draft. AB and AT revised the draft with critical inputs from all authors.

Data availability

The maximum and minimum temperature data is available from https://www.imdpune.gov.in/Clim_Pred_LRF_New/Grided_Data_Download.html. The bias-corrected CMIP6 model data is from Mishra *et al.* (2020) and is available from Zenodo (https://zenodo.org/record/3874046#.Y2IWJnZBxQ8).

References

Babu S S, Manoj M, Moorthy K K, Gogoi M M, Nair V S, Kompalli S K, Satheesh S, Niranjan K, Ramagopal K, Bhuyan P K and Singh D 2013 Trends in aerosol optical depth over Indian region: Potential causes and impact indicators; *J. Geophys. Res. Atmos.* **118**(**20**) 11,794–11,806.

Bhatla R, Pant M, Singh D, Verma S and Mandal B 2020 Evaluation of cold wave events over Indo-Gangetic Plain in India; *J. Agrometeorol.* **22**(**2**) 233–238.

Bitencourt D P, Fuentes M V, Franke A E, Silveira R B and Alves M P A 2020 The climatology of cold and heat waves in Brazil from 1961 to 2016; *Int. J. Climatol.* **40**(**4**) 2464–2478.

Cheng J, Xu Z, Bambrick H, Prescott V, Wang N, Zhang Y, Su H, Tong S and Hu W 2019 Cardiorespiratory effects of heatwaves: A systematic review and meta-analysis of global epidemiological evidence; *Environ. Res.* **177(108610)**.

Chowdhury B 2022 Trends, intensification, attribution and uncertainty of projected heatwaves in India; *Int. J. Climatol.* 1–20, https://doi.org/10.1002/joc.7665.

Das J and Umamahesh N V 2022 Heat wave magnitude over India under changing climate: Projections from CMIP5 and CMIP6 experiments; *Int. J. Climatol.* **42**(**1**) 331–351.

Dash S and Mamgain A 2011 Changes in the frequency of different categories of temperature extremes in India; *J. Appl. Meteorol. Climatol.* **50**(**9**) 1842–1858.

Dave P, Bhushan M and Venkataraman C 2020 Absorbing aerosol influence on temperature maxima: An observation based study over India; *Atmos. Environ.* **223** 117237.

De U S and Mukhopadhyay R K 1998 Severe heat wave over the Indian subcontinent in 1998, in perspective of global climate; *Curr. Sci.* **75**(**12**) 1308–1311.

Dimri A P and Chevuturi A 2014 Model sensitivity analysis study for western disturbances over the Himalayas; *Meteorol. Atmos. Phys.* **123**(**3**) 155–180.

Fu S H, Gasparrini A, Rodriguez P and Jha P 2018 Mortality attributable to hot and cold ambient temperatures in India: A nationally representative case-crossover study; *PLoS Med.* **15**(**7**) e1002619.

Hirsch A L, Ridder N N, Perkins-Kirkpatrick S E and Ukkola A 2021 CMIP6 multi-model evaluation of present-day heatwave attributes; *Geophys. Res. Lett.* **48**(**22**) e2021GL095161.

Hunt K M, Turner A G and Shaffrey L C 2019 Falling trend of western disturbances in future climate simulations; *J. Clim.* **32**(**16**) 5037–5051.

IPCC 2021 Climate change 2021: The physical science basis. Contribution of Working Group I to the Sixth Assessment Report of the Intergovernmental Panel on Climate Change, Cambridge University Press, Cambridge, United Kingdom and New York, NY, USA.

Jenamani R 2012 Analysis of ocean-atmospheric features associated with extreme temperature variation over east coast of India – A special emphasis to Orissa heat waves of 1998 and 2005; *MAUSAM* **63**(**3**) 401–422.

Kumar P and Sarthi P P 2019 Surface temperature evaluation and future projections over India using CMIP5 models; *Pure Appl. Geophys.* **176**(**11**) 5177–5201.

Lu L, Wang Z and Shi P 2015 Mapping cold wave risk of the world, World Atlas of Natural Disaster Risk, Springer, pp. 189–207.

Ma S and Zhu C 2019 Extreme cold wave over East Asia in January 2016: A possible response to the larger internal atmospheric variability induced by Arctic warming; *J. Clim.* **32**(**4**) 1203–1216.

Mahdi S S and Dhekale B S 2016 Long term climatology and trends of heat and cold waves over southern Bihar, India; *J. Earth Syst. Sci.* **125**(**8**) 1557–1567.

Mazdiyasni O, AghaKouchak A, Davis S J, Madadgar S, Mehran A, Ragno E, Sadegh M, Sengupta A, Ghosh S and Dhanya C J S 2017 Increasing probability of mortality during Indian heat waves; *Sci. Adv.* **3**(**6**) e1700066.

Mishra V, Mukherjee S, Kumar R and Stone D A 2017 Heat wave exposure in India in current, 1.5°C, and 2.0°C worlds; *Environ. Res. Lett.* **12**(**12**) 124012.

Mishra V, Bhatia U and Tiwari A D 2020 Bias-corrected climate projections for South Asia from Coupled Model Intercomparison Project-6; *Sci. Data* **7**(**1**) 338.

Mondal A, Sah N, Sharma A, Venkataraman C and Patil N 2021 Absorbing aerosols and high-temperature extremes in India: A general circulation modelling study; *Int. J. Climatol.* **41**(**S1**) E1498–E1517.

Nairn J R and Fawcett R J B 2015 The excess heat factor: A metric for heatwave intensity and its use in classifying heatwave severity; *Int. J. Environ. Res. Public Health* **12**(**1**) 227–253.

Namroodi M, Hamidianpour M and Poodineh M 2021 Spatio-temporal analysis of changes in heat and cold waves across Iran over the statistical period 1966–2018; *Arab. J. Geosci.* **14**(**10**) 1–14.

Pai D S and Nair S 2022 Impact of El-Niño-Southern Oscillation (ENSO) on extreme temperature events over India; *MAUSAM* **73**(**3**) 597–606.

Pai D, Srivastava A and Nair S A 2017 Heat and cold waves over India, observed climate variability and change over the Indian Region, Springer, pp. 51–71.

Piticar A, Croitoru A E, Ciupertea F A and Harpa G-V 2018 Recent changes in heat waves and cold waves detected based on excess heat factor and excess cold factor in Romania; *Int. J. Climatol.* **38**(**4**) 1777–1793.

Ratnam J, Behera S K, Ratna S B, Rajeevan M and Yamagata T 2016 Anatomy of Indian heatwaves; *Sci. Rep.* **6**(**1**) 1–11.

Ray K, Giri R, Ray S, Dimri A and Rajeevan M 2021 An assessment of long-term changes in mortalities due to extreme weather events in India: A study of 50 years' data, 1970–2019; *Wea. Clim. Extrem.* **32(100315)**.

Rohini P, Rajeevan M and Srivastava A K 2016 On the variability and increasing trends of heat waves over India; *Sci. Rep.* **6**(**1**) 1–9.

Sandeep A and Prasad V S 2020 On the variability of cold wave episodes over Northwest India using an NGFS retrospective analysis; *Pure Appl. Geophys.* **177**(**2**) 1157–1166.

Saranya J S, Roxy M K, Dasgupta P and Anand A 2022 Genesis and trends in marine heatwaves over the Tropical Indian Ocean and their interaction with the Indian Summer Monsoon; *J. Geophys. Res.: Oceans* **127(2)** e2021JC017427.

Spinoni J, Lakatos M, Szentimrey T, Bihari Z, Szalai S, Vogt J and Antofie T 2015 Heat and cold waves trends in the Carpathian Region from 1961 to 2010; *Int. J. Climatol.* **35**(**14**) 4197–4209.

Srivastava A, Rajeevan M and Kshirsagar S R 2009 Development of a high resolution daily gridded temperature data set (1969–2005) for the Indian region; *Atmos. Sci. Lett.* **10**(**4**) 249–254.

Thomas A, Sarangi C and Kanawade V P 2019 Recent increase in winter hazy days over Central India and the Arabian Sea; *Sci. Rep.* **9**(**1**) 17406.

Unkašević M and Tošić I 2015 Seasonal analysis of cold and heat waves in Serbia during the period 1949–2012; *Theor. Appl. Climatol.* **120** 29–40, https://doi.org/10.1007/s00704-014-1154-7.

Van Oldenborgh G J, Mitchell-Larson E, Vecchi G A, De Vries H, Vautard R and Otto F 2019 Cold waves are getting milder in the northern midlatitudes; *Environ. Res. Lett.* **14**(**11**) 114004.

Corresponding editor: P A Francis